Bull. Mater. Sci., Vol. 39, No. 6, October 2016, pp. 1507–1513. © Indian Academy of Sciences.
DOI 10.1007/s12034-016-1294-8

Photocatalytic degradation of methylene blue by C_3N_4/ZnO: the effect of the melamine/ZnO ratios

PONGSATON AMORNPITOKSUK[1,2,*], SUMETHA SUWANBOON[3], URAIWAN SIRIMAHACHAI[1], CHAMNAN RANDORN[4] and KASIDID YAEMSUNTHORN[4]

[1]Department of Chemistry, Faculty of Science, Prince of Songkla University, Hat-Yai, Songkhla 90112, Thailand
[2]Center of Excellence for Innovation in Chemistry, Faculty of Science, Prince of Songkla University, Hat-Yai, Songkhla 90112, Thailand
[3]Department of Materials Science and Technology, Faculty of Science, Prince of Songkla University, Hat-Yai, Songkhla 90112, Thailand
[4]Department of Chemistry, Faculty of Science, Chiang Mai University, Chiang Mai 50200, Thailand

MS received 18 November 2015; accepted 4 April 2016

Abstract. **The C_3N_4/ZnO composite photocatalysts were synthesized by mechanical milling combined with a calcination process. Various ratios of melamine and ZnO powders were milled by a planetary ball mill for 10 h. After heating at 540°C for 3 h in air, melamine was converted to C_3N_4 but the formation of C_3N_4 depended on the ratios of the melamine and ZnO (M/Z) powders. From the experimental results, the conversion of melamine to C_3N_4 could be inhibited by ZnO particles; as there was no detectable C_3N_4 in the sample at low M/Z values or high ZnO contents. The photocatalytic activities of prepared samples were investigated under the illumination of blacklight and fluorescent lamps as the low wattage light source. The C_3N_4/ZnO showed a better photocatalytic activity than ZnO to degrade a methylene blue (MB) dye solution using blacklight lamps, but there is no significant difference in photocatalytic activities between ZnO and prepared C_3N_4/ZnO under visible light by the fluorescent lamps. However, the prepared C_3N_4/ZnO can well function under illumination by Xe lamp as the high power light source. Ecotoxicities of MB solutions before and after photocatalytic process were also studied through growth inhibition of the alga *Chlorella vulgaris*.**

Keywords. **C_3N_4; ZnO; thermal pyrolysis; photocatalysis; ecotoxicity.**

1. Introduction

The textile industry is one of the largest industries, which globally and annually produces a large amount of wastewater containing many toxic chemical dyes. For environmental concern, there is a need to develop effective and cheap treatment methods to treat the wastewater before it is discharged into the environment. Many methods have been developed to decolourize the textile wastewater such as adsorption, chemical coagulation, oxidization and so on [1–3]. Photocatalysis is one of the most effective treatment processes that has drawn increasing attention over the last few decades, and one of the most popular photocatalyst used is ZnO because of its high activity, low cost and environmental friendliness [4]. However, the efficiency of ZnO is reduced by the charge recombination that occurs inside the ZnO particles during photocatalysis [5,6]. In order to inhibit this phenomenon, many researchers have tried to combine ZnO with metals to form a heterostructure that will separate photoelectrons and holes, leading to a reduction of the charge recombination and thus an increase in the photocatalytic activity. From the literature, good coupling of metals has been reported for silver (Ag) [5,6], but it is an expensive metal. Hence, many research groups have tried to find a cheaper coupling material. One of the possible low-cost coupling material is C_3N_4, as it is inexpensive, chemically stable and non-toxic [7].

The C_3N_4/ZnO can be prepared by two main methods. The first route for the individual preparations of C_3N_4 and ZnO powders follows combining C_3N_4 and ZnO together by mechanical or chemical methods [8–10]. The second method is a solution process starting with a precursor of C_3N_4, such as melamine and the Zn^{2+} ions that are mixed together in the solution and the mixture then undergoes calcination to obtain C_3N_4/ZnO [11,12]. However, as far as we know there has been no report about the combination of ZnO with melamine using a mechanical milling (MM) method following the calcination process. This process has many advantages such as the possibility of large-scale production, the use of no other chemicals and production of a low waste from the process, including the cleaning process.

In this study, the C_3N_4/ZnO was prepared by the MM of melamine and ZnO powders coupled to the calcination process. It also describes the studies on the effect of

*Author for correspondence (ampongsa@yahoo.com, pongsaton.a@psu.ac.th)

the melamine/ZnO (M/Z) ratios on the formation of the C_3N_4/ZnO. The photocatalytic activities of prepared samples were tested through the degradation of a methylene blue (MB) dye solution under black light and visible light irradiations. Furthermore, the ecotoxicities of treated and untreated MB solutions were evaluated by the growth inhibition test with *Chlorella vulgaris*.

2. Experimental

The C_3N_4/ZnO was prepared through a combination of MM and calcinations. MM was performed in a planetary mill with a Si_3N_4 vial and balls. The ball-to-powder weight ratio was kept at 10:1. The weight ratios between the melamine and the ZnO powders were varied at 0.5:0.01, 0.5:0.05, 0.5:0.1, 0.5:0.2, 0.5:0.3 and 0.5:0.5. The milling was operated at 350 rpm and was stopped every 30 min in order to prevent rapid engine wear. After milling for 10 h, the powders were placed in an alumina crucible with a cover for decreasing the sublimation of melamine and treated at the required temperatures for 3 h at 5°C min^{-1}.

The phase identification and morphology of the samples were investigated by X-ray diffractometer (XRD, X'Pert MPD, Philips) using CuK_α radiation at a wavelength of 0.15406 nm and a transmission electron microscope (JEM 2010, JEOL), respectively. The elemental distribution of N and Zn on the surface of the sample was examined using a scanning electron microscopy (Quanta400, FEI) equipped with an energy-dispersive spectroscopy (EDS). The carbon and nitrogen contents in the samples were determined by a CHNS-O Analyzer (Flash EA 1112 Series, Thermo Quest). The absorption spectra of the samples were measured by a UV-VIS diffuse reflectance spectrophotometer (UV2450, Shimadzu) using $BaSO_4$ as the reference.

The photocatalytic activity of the prepared samples was studied through the degradation of MB solution. In the typical procedure, 150 mg of the sample powders were added into 150 ml of 1×10^{-5} M MB solution. The mixture was stirred in the dark for 30 min to ensure that the adsorption/desorption was in equilibrium. The mixture was then irradiated under blacklight by three parallel blacklight fluorescent tubes (Sylvania, 18 W), or under visible light by three parallel fluorescent tubes (T8 Philips, 18W, cover with 420 nm longpass filter) or Xe lamp (Osram 300 W, cover with 420 nm longpass filter) and the solution was filtered and centrifuged after the mixture was irradiated for 3 h. The remaining MB concentrations were determined by a UV-VIS spectrophotometer (UV2600, Shimadzu) and the degradation (%) was calculated by the following equation:

$$\text{Degradation}(\%) = [(A_o - A_t)/A_o] \times 100,$$

where A_o and A_t are the absorbances of the MB solution before irradiation and after irradiation for 3 h.

The ecotoxicities of MB solutions before and after photocatalysis were investigated through an inhibitory growth of *C. vulgaris* as a bioindicator. The *C. vulgaris* cultures inoculated with 8×10^5 cells ml^{-1} were introduced in each flask containing 100 ml of the required solutions (deionized, treated and untreated MB solutions). The flasks were shaken at 150 rpm at a constant temperature of 25 ± 2°C and then illuminated by white fluorescent light (18 W) following a day/night rhythm of 12/12 h for 10 days. The cell density was evaluated by counting *C. vulgaris* cells with haemacytometer slide. The relative individual cells were calculated by the following equation:

$$\begin{aligned}\text{Relative individual cell} = {} & \{[(\#\text{ at days } 3, 5 \text{ or } 10) \\ & -(\#\text{ at day } 1)]/(\#\text{ at day } 1)\} \\ & \times 100,\end{aligned}$$

where # is the number of individual cells of *C. vulgaris*.

3. Results and discussion

3.1 *Effect of ratio between melamine and ZnO for C_3N_4/ZnO formation*

The selected weight ratios between melamine and commercial ZnO (M/Z ratios) were 50, 10, 5, 2.5, 1.67 and 1. After the mixtures were milled for 10 h and then calcined at 540°C for 3 h, the XRD patterns of the resulting products were observed, as shown in figure 1. The amount of C_3N_4 in the sample is decreased with an increase in the ZnO loading (or decrease in M/Z ratio), indicating a reduction in the peak intensity of C_3N_4 as presented in figure 1. At the M/Z ratio of less than 5, C_3N_4 was not detected in the XRD patterns. In this study, the melamine content was kept at 0.5 g for all experiments so the absence of diffraction peaks of C_3N_4 for samples at the M/Z ratio =1

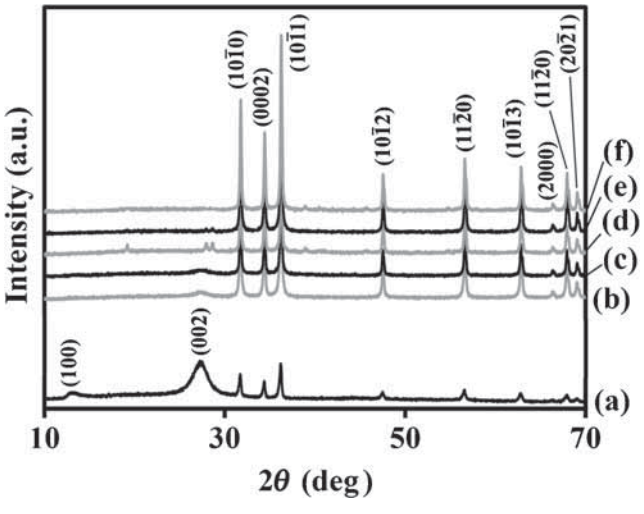

Figure 1. XRD patterns of samples at the M/Z ratios of (a) 50, (b) 10, (c) 5, (d) 2.5, (e) 1.67 and (f) 1, after being calcined at 540°C for 3 h in air. The three and four Miller indices correspond to the C_3N_4 and ZnO phases, respectively.

did not come from the small amount of C_3N_4 that was not detected by the XRD technique. Furthermore, the results of the elemental analysis for the calcined samples, as presented in table 1, confirmed the absence of melamine from the system and further suggested that the melamine did not transform to a non-crystalline substance that was not detectable by the XRD technique.

To prove that the loss of melamine did not come from the oxygen contained in the system, the sample at $M/Z = 1$ was calcined at 540°C for 3 h in N_2 atmosphere. The resulting product showed only diffraction peaks of pure ZnO, as presented in figure 2. This confirmed that the absence of C_3N_4 in this sample did not come from the reaction with oxygen contained in the crucible.

Another reason for the absence of melamine was that the sublimation of melamine. In fact, the melamine sublimates and thermal condenses to intermediate products such as melam, melem and melon at 297–390°C [13]. To prove this hypothesis, the sample with the $M/Z = 1$ was heated over the temperature range of 300–500°C. Figure 3 shows the effect of the calcination temperature on C_3N_4 formation for sample at $M/Z = 1$. It is obvious that the XRD patterns still showed the diffraction peaks that corresponded to melamine and ZnO when the sample was calcined at 300°C for 3 h. The presence of melamine at temperatures lower than 300°C has been detected previously as reported in the literature [13]. However, at 350°C, the sample at $M/Z = 1$ showed that there were two powder groups in the crucible (upper inner sidewall and bottom of crucible), as shown in supplementary figure S1. This evidence can be found in the case of pure melamine. For both systems ($M/Z = 1$ and pure melamine), the deposited crystals at the upper inner sidewall of the crucible showed the XRD pattern that corresponded to melamine, as shown in figure 4c. The XRD pattern of the powder presents at the bottom of crucible for sample at

Table 1. Elemental analysis results of samples at various M/Z ratios after being calcined at 540°C for 3 h in air.

M/Z	N (wt%)	C (wt%)	N/C (atomic)
50	52.48 ± 0.33	30.41 ± 0.20	1.48
10	36.52 ± 0.57	21.39 ± 0.32	1.46
5	22.30 ± 0.17	13.16 ± 0.17	1.45
2.5	7.52 ± 0.06	4.04 ± 0.01	—
1.67	2.38 ± 0.07	1.46 ± 0.09	—
1	0	0	—

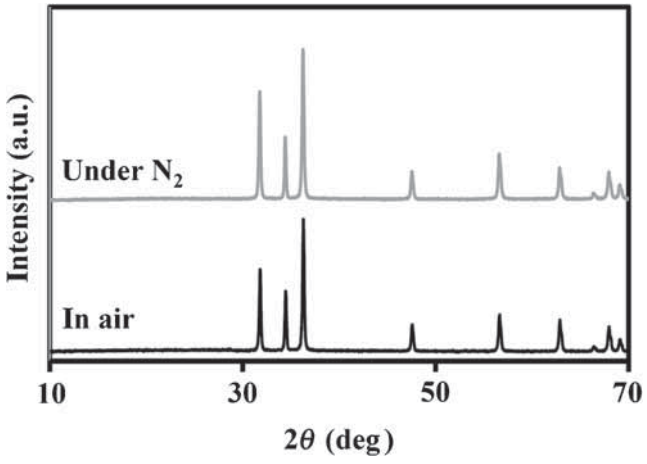

Figure 2. XRD patterns of samples at the M/Z ratio of 1, after being calcined at 540°C for 3 h in air and in N_2 atmosphere.

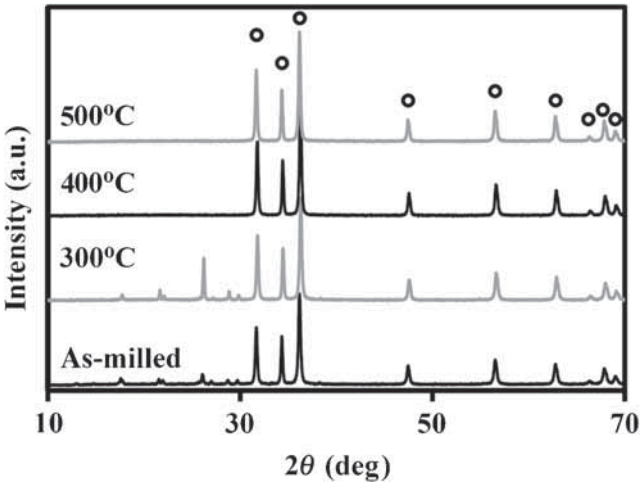

Figure 3. XRD patterns of samples at the M/Z ratio of 1 before and after being calcined at various temperatures for 3 h in air. The circle symbols represent ZnO phase.

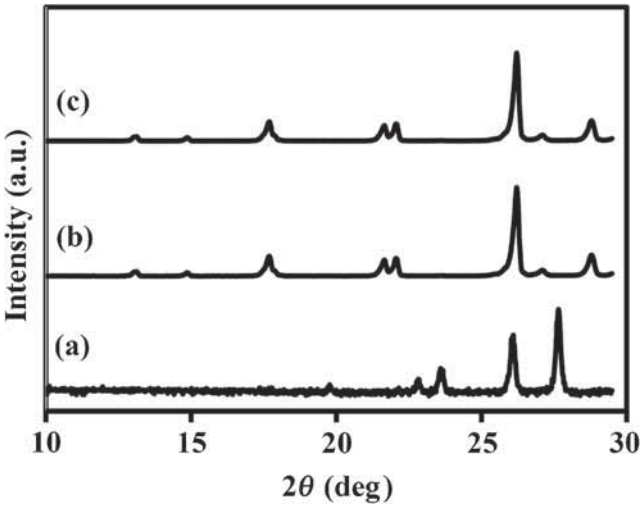

Figure 4. XRD patterns of powder at the bottom of the crucible for samples at (a) $M/Z = 1$ as well as (b) pure melamine and (c) the typical XRD of the powder at the upper inner sidewall of the crucible for samples at $M/Z = 1$ and pure melamine. The samples were heated at 350°C for 3 h.

$M/Z = 1$ was assigned to ZnO (supplementary figure S2) as the major phase. The diffraction pattern of secondary phase presenting in this sample recording in the range of 2θ = 10–30° (figure 4a) showed several peaks that were different from that of pure melamine. On the other hand, the powder in the bottom of the crucible for the calcined pure melamine showed the XRD pattern that corresponded to melamine only (figure 4b). So, at 350°C, the ZnO in the melamine facilitated the sublimation of melamine and this probably leads to further inhibit the thermal condensation of melamine to an intermediate phase. At 400 and 500°C, there was no crystal deposit at the upper inner sidewall of the crucible, and the XRD pattern of the calcined sample at $M/Z = 1$ showed only the diffraction peaks of ZnO as seen in figure 3. It is possible that the ZnO inhibited the thermal condensation of the melamine, so melamine was decomposed by heat hence its loss from the system. This evidence occurred when the sample at $M/Z = 1$ was mixed by hand and calcination at 540°C for 3 h (data are not shown). Furthermore, the sample at $M/Z = 1$ after being heated to 540°C at a heating rate of 5°C min^{-1} followed by immediately quenching to the room temperature showed the XRD pattern that corresponded to pure ZnO (data are not shown).

As ZnO shows the catalytic decomposition phenomena, it is possible that the loss of melamine could come from this reaction. To ensure that ZnO does not catalyse the decomposition of melamine, the ZnO was replaced by Na_2CO_3 (weight ratio of melamine: Na_2CO_3 = 1:1) in order to prove this hypothesis. The resulting data indicated that only Na_2CO_3 was presented in XRD pattern and there was no diffraction peak that corresponded to the C_3N_4, as shown in figure 5. This confirmed that the solid particles can inhibit the thermal condensation of melamine to form C_3N_4 and the loss of melamine in the system probably came from self-thermal decomposition.

The TEM image of pure C_3N_4 after being calcined for 3 h in air shows irregular and larger plates (figure 6a) as was usually observed in the bulk C_3N_4 [14]. However, for sample at $M/Z = 10$, the solid particles that were partially covered with a thin sheet of C_3N_4, as presented in figure 6b, exhibited a d spacing of 0.259 nm corresponding to (0002) for ZnO, as shown in figure 6c. The elemental analysis from spectra 1 (Zn = 55 at.% and O = 45 at.%) and 2 (C = 41 at.% and N = 59 at.%), as obtained in figure 7a, confirmed a heterostructure of C_3N_4/ZnO. For EDS mapping, as presented in figure 7b–d, there was a small amount of ZnO spread on the surface of C_3N_4 for sample at $M/Z = 50$. The C_3N_4 contents in the products were also decreased with a reduction of the M/Z value and it was in agreement with the results from XRD patterns (figure 1). The UV-VIS diffuse reflectance spectra of all samples are shown in figure 8. The absorption peak at 395 nm comes from the electron transition between the highest occupied molecular orbital (HOMO) and the lowest unoccupied molecular orbital (LUMO) in the C_3N_4 [15]. This peak decreased when the M/Z ratios were

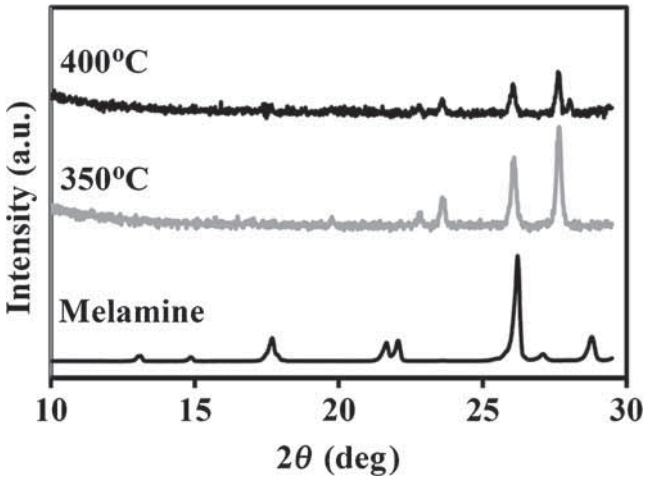

Figure 5. XRD patterns of samples containing 0.5 g of melamine and 0.5 g of Na_2CO_3 after being calcined at different temperatures for 3 h. For 350°C, it is an XRD of powder in the bottom of crucible.

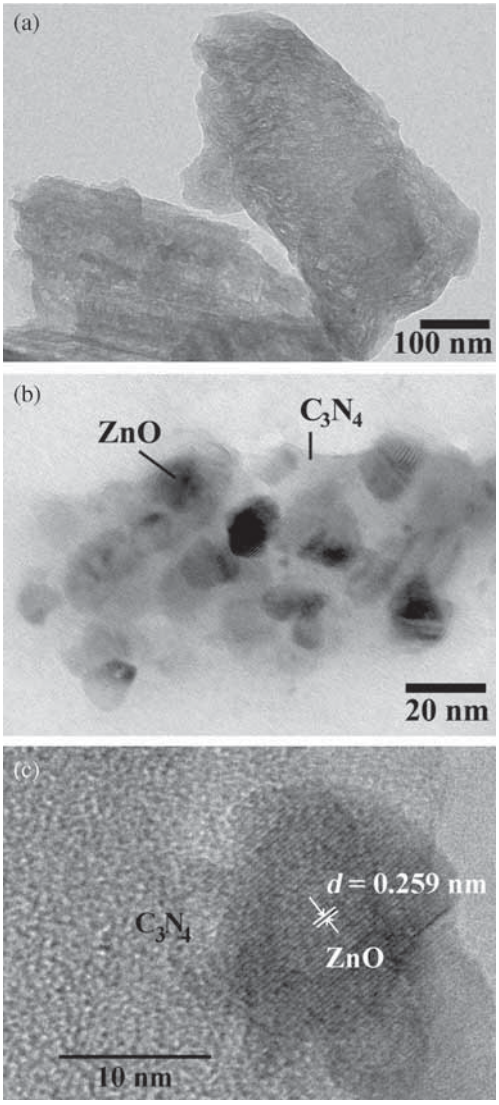

Figure 6. TEM images of (**a**) pure C_3N_4 and (**b**) sample at the M/Z ratio of 10, and (**c**) HR-TEM image of sample at the M/Z ratio of 10.

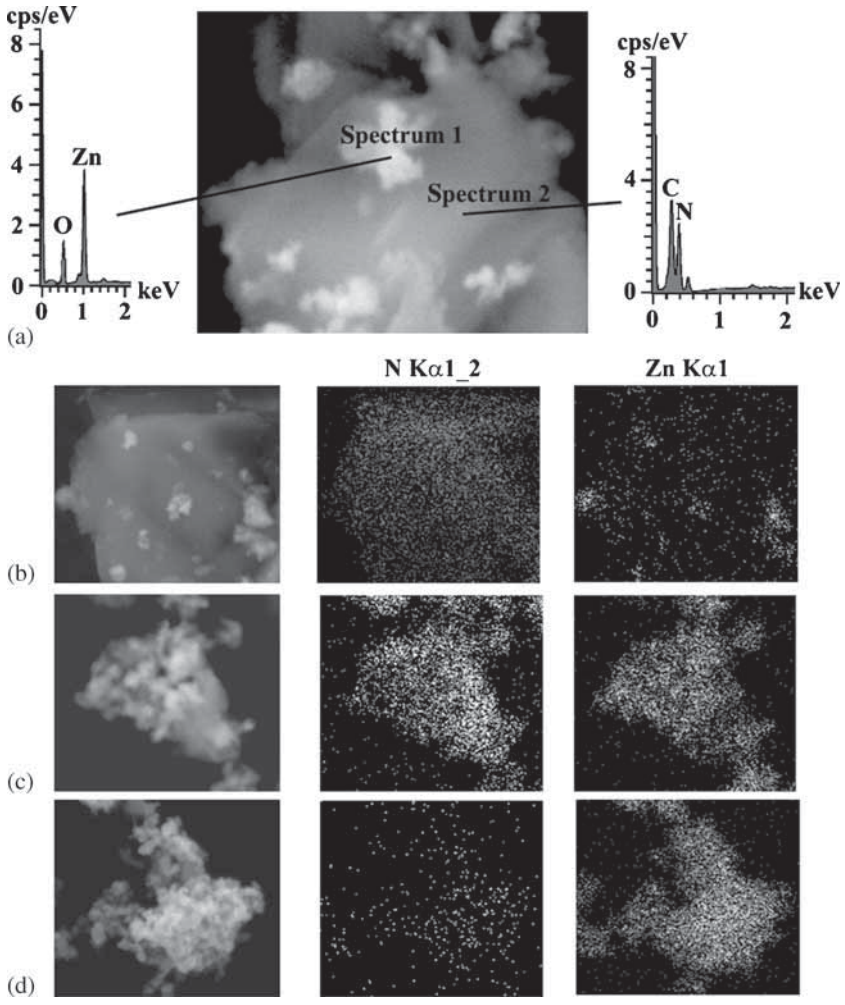

Figure 7. The corresponding (**a**) EDS spectra of C_3N_4/ZnO and EDS mapping of samples at M/Z ratios of (**b**) 50, (**c**) 5 and (**d**) 2.5, after being calcined at 540°C for 3 h in air.

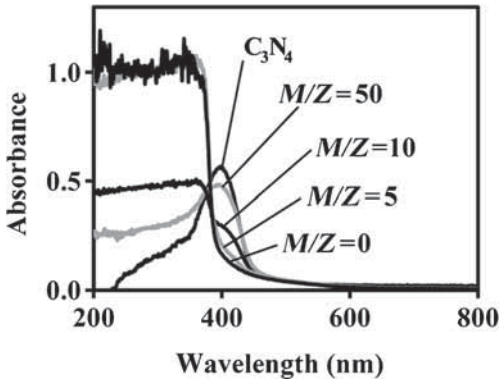

Figure 8. Absorption spectra of pure C_3N_4 and the samples at M/Z ratios of 50, 10, 5 and 0 (pure ZnO) after being calcined at 540°C for 3 h in air.

changed from 50 to 0 (pure ZnO), because of the reduction of the C_3N_4 contents in the C_3N_4/ZnO. The absorption in the UV region was attributed to the ZnO that increased with decreased M/Z ratios.

3.2 *Photocatalytic activity under blacklight*

The photocatalytic degradations of MB dye solutions for all samples as photocatalysts are presented in figure 9. For blacklight illumination, the photocatalytic activity of pure C_3N_4 is very poor and the same has also been regularly reported in the literature [16]. At the $M/Z = 50$, there was some ZnO in the sample that absorbs photons, so the photocatalytic activity of this sample was higher than that of the pure C_3N_4. The maximum activity was found at $M/Z = 10$, as shown in figure 9. After this point (for $M/Z = 5$), the photocatalytic activity decreased because of the low C_3N_4 on the surface of the ZnO. However, its activity is still higher than that of pure ZnO. At the $M/Z = 2.5$, there was some decomposed substance on the surface of the ZnO, as seen in figure 1d, and this could reduce its activity. At the $M/Z = 1.67$, the photocatalytic activity increased again because the content of the decomposed substance on the surface of ZnO was lower, as observed in figure 1e. At the $M/Z = 1$ in air, the impurity phase was not found in this sample and its activity was nearly identical to that of pure

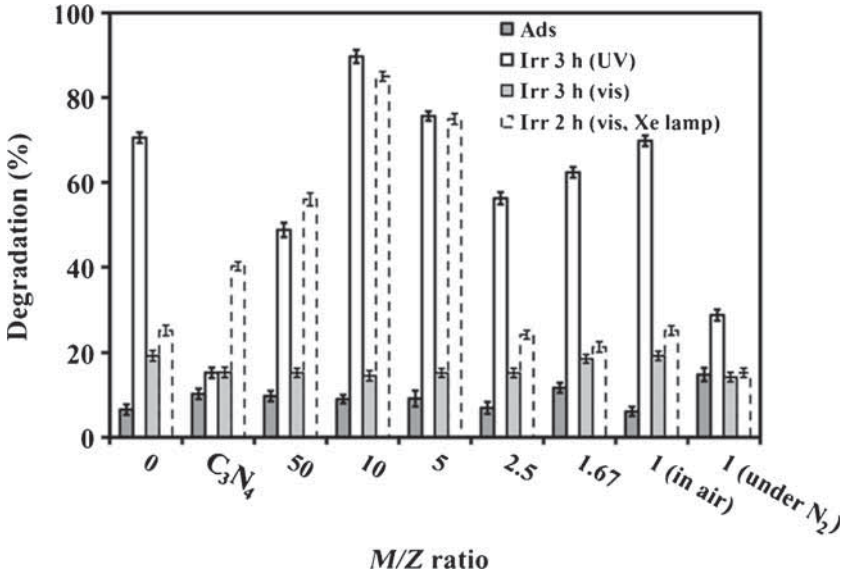

Figure 9. Photocatalytic activity of pure C_3N_4 and samples at the M/Z ratios of 0, 50, 10, 5, 2.5, 1.67 and 1, after being calcined at 540°C for 3 h in air. The last one is the photocatalytic activity of the sample at the M/Z ratio of 1 after being calcined at 540°C for 3 h in N_2. $M/Z = 0$ refers to pure ZnO.

ZnO ($M/Z = 0$). On the other hand, the sample at $M/Z = 1$ in N_2 atmosphere showed the worst activity compared with the other samples. This could result from the impurity that cannot be oxidized completely in N_2 atmosphere and this phase cannot be detected by the XRD technique.

Under UV rays, after the ZnO absorbs the photons that have energies equal to or greater than its bandgap, the electrons make transition from the valence band to the conduction band and leave holes in the valence band. Holes in the valence band of the ZnO can migrate to the HOMO levels of C_3N_4 and produce the charge separation and this reduces the probability of charge recombination between the photoelectrons and the holes, leading to an increase in the photocatalytic activity [16]. Furthermore, C_3N_4 can reduce the probability of the photoinduced dissolution of ZnO. The photocorrosion by ZnO can be described as follows [17]:

$$\mathrm{ZnO} + 2\mathrm{h}^+ + n\mathrm{H_2O} \rightarrow \mathrm{Zn(OH)}_n^{(n-2)+} + 1/2\mathrm{O_2} + n\mathrm{H}^+.$$

In C_3N_4/ZnO, under UV rays, the holes in the valence band of ZnO could transfer to the HOMO of the C_3N_4 as mentioned above and the rate of photocorrosion will be inhibited.

3.3 *Photocatalytic activity under visible light*

Under visible light illumination using the low wattage fluorescent lamps, all prepared samples showed very poor photocatalytic degradation of MB dye solution, but their photocatalytic activities were improved when the low wattage fluorescent lamps were replaced by a 300 W Xe lamp, as shown in figure 9. It is clearly observed that the photocatalytic activity was in order of $M/Z = 10 > M/Z = 5 > M/Z = 50 >$ pure $C_3N_4 > M/Z = 0$ (pure ZnO). The photocatalytic activity of pure C_3N_4 was higher than that of pure ZnO ($M/Z = 0$) because the C_3N_4 has a lower bandgap than ZnO. In fact, the photocatalytic activity of C_3N_4 comes from the $^{\cdot}O_2^-$ radicals because the holes in the HOMO of the C_3N_4 cannot oxidize OH^- to $^{\bullet}OH$, as the HOMO of C_3N_4 (1.57 eV *vs.* NHE) is more negative than the standard redox potential $E^\circ(^{\bullet}OH/OH^-)$ (1.99 eV *vs.* NHE), while the LUMO of C_3N_4 (−1.12 eV *vs.* NHE) is more negative than the standard redox potential $E^\circ(O_2/^{\bullet}O_2^-)$ (−0.33 eV *vs.* NHE) [18] so the $^{\bullet}O_2^-$ radicals can be generated. The presence of C_3N_4 in ZnO can enhance the photocatalytic degradation of MB and the best activity was found at $M/Z = 10$, as shown in figure 9. Under visible light, electrons in HOMO of C_3N_4 absorb photons and promote to its LUMO, and then transfer to conduction band of ZnO generating the charge separation. These electrons would react with oxygen species to form $^{\bullet}O_2^-$ that can oxidize the dye molecules. For the samples $M/Z = 1$ to $M/Z = 2.5$, there were no C_3N_4 in the samples, as shown in figure 1, so the photocatalytic activities of these samples and pure ZnO were not significantly different, as shown in figure 9.

3.4 *Ecotoxicity of degraded products from photocatalysis*

Using $M/Z = 10$ as photocatalyst, the MB solutions after 4 h of visible light (Xe lamp) and blacklight illuminations have the total carbon contents of 0.25 and 0.20%, respectively. Although these values are lower than that of initial MB solution (0.95%), they are not equal to zero indicating that there are some residual organic molecules, which probably are more toxic than parent dye molecules. So, the

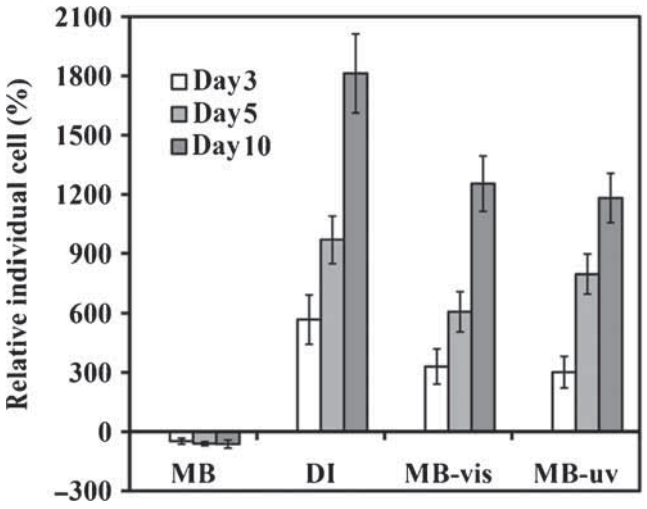

Figure 10. *C. vulgaris* growth in MB solution (MB), deionized (DI), treated MB solutions under visible light using Xe lamp (MB-vis) and blacklight (MB-uv).

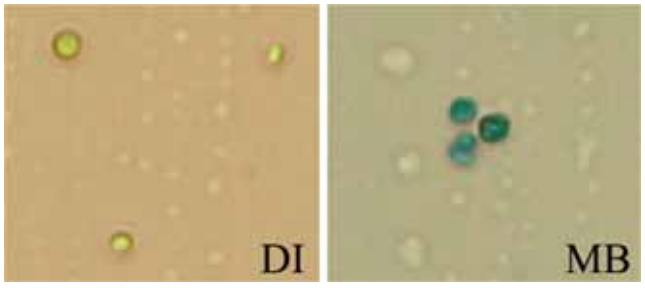

Figure 11. Optical micrographs of *C. vulgaris* treated with deionized water (control) and MB solution.

ecotoxicities of treated and untreated MB solutions were investigated through a growth of *C. vulgaris* as a bioindicator. Figure 10 shows the relative individual cells after exposure to treated and untreated MB solutions. Results clearly showed that the MB molecules were more toxic to *C. vulgaris* than the degraded products. MB can penetrate or uptake into *C. vulgaris* cell as the colour of the cytoplasm changes from green to blue, as presented in figure 11, and this probably causes cell growth inhibition.

4. Conclusion

C_3N_4/ZnO was successfully synthesized through a combination of ZnO and melamine powders produced by the milling method and coupled with the calcination process. The ratio between melamine and ZnO (M/Z) had a strong effect on the C_3N_4/ZnO formation. From the experimental results, the conversion of melamine to C_3N_4 could be inhibited by ZnO particles or ZnO could facilitate the thermal combustion of melamine, so the C_3N_4 cannot be produced in an environment with a high ZnO content. Furthermore, the C and N contents also decreased with an increment of the ZnO contents and this confirmed the loss of melamine or C_3N_4 in the samples. In this study, the sample prepared from the $M/Z = 10$ showed the best photocatalytic degradation of MB dye solution under blacklight irradiation and it was much more efficient than that of pure ZnO. The low wattage light sources cannot activate the electron transition in C_3N_4, so C_3N_4/ZnO showed very poor photocatalytic properties. However, it can function well under the illumination of the high power light source. Using *C. vulgaris* as bioindicator, the degraded products are less toxic than MB dye molecules. MB can penetrate into *C. vulgaris* cell that probably causes cell growth inhibition.

Acknowledgements

We would like to acknowledge the Center of Excellence for Innovation in Chemistry (PERCH-CIC), Office of the Higher Education Commission, Ministry of Education. We would also like to thank Dr Brian Hodgson for assistance with the English.

References

[1] Palma-Goyes R E, Silva-Agredo J, González I and Torres-Palma R A 2014 *Electrochim. Acta* **140** 427
[2] Yao T, Guo S, Zeng C, Wang C and Zhang L 2015 *J. Hazard. Mat.* **292** 90
[3] Chafi M, Gourich B, Essadki A H, Vial C and Fabregat A 2011 *Desalination* **281** 285
[4] Darroudia M, Sabouric Z, Oskuee R K, Zak A K, Kargar H and Hamid M H N A 2014 *Cer. Inter.* **40** 4827
[5] Ren C, Yang B, Wu M, Xu J, Fu Z, lv Z, Guo T, Zhao Y and Zhu C 2010 *J. Hazard. Mat.* **182** 123
[6] Zheng Y, Zheng L, Zhan Y, Lin X, Zheng Q and Wei K 2007 *Inorg. Chem.* **46** 6980
[7] Goglio G, Foy D and Demazeau G 2008 *Mat. Sci. Eng. R* **58** 195
[8] Liu W, Wang M, Xu C, Chen S and Fu X 2013 *J. Mol. Catal. A* **368–369** 9
[9] Li X, Li M, Yang J, Li X, Hu T, Wang J, Sui Y, Wu X and Kong L 2014 *J. Phys. Chem. Solids* **75** 441
[10] Zhou J, Zhang M and Zhu Y 2014 *Phys. Chem. Chem. Phys.* **16** 17627
[11] Liu W, Wang M, Xu C and Chen S 2012 *Chem. Eng. J.* **209** 386
[12] Sun J X, Yuan Y P, Qiu L G, Jiang X, Xie A J, Shen Y H and Zhu J F 2012 *Dalton Trans.* **41** 6756
[13] Dong G, Zhang Y, Pan Q and Qiu J 2014 *J. Photochem. Photobiol. C: Photochem Rev.* **20** 33
[14] Zhang L, Liu D, Guan J, Chen X, Guo X, Zhao F, Hou T and Mu X 2014 *Mat. Res. Bull.* **59** 84
[15] Wang C, Zhu W, Xu Y, Xu H, Zhang M, Chao Y, Yin S, Li H and Wang J 2014 *Cer. Inter.* **40** 11627
[16] Chen D, Wang K, Xiang D, Zong R, Yao W and Zhu Y 2014 *Appl. Catal. B: Environ.* **147** 554
[17] Rudd A L and Breslin C B 2000 *Electrochim. Acta* **45** 1571
[18] Wang Y, Shi R, Lin J and Zhu Y 2011 *Energy Environ. Sci.* **4** 2922